LUND UNIVERSITY

Experimental oscillator strengths for forbidden lines in complex spectra

Hartman, Henrik; Johansson, Sveneric; Lundberg, Hans; Lundin, P; Mannervik, S; Schef, P

Link to publication

Experimental Oscillator Strengths for Forbidden Lines in Complex Spectra

Experimental Oscillator Strengths for Forbidden Lines in Complex Spectra

H. Hartman[1,*], S. Johansson[1], H. Lundberg[2], P. Lundin[3], S. Mannervik[3] and P. Schef[3]

[1]Atomic Astrophysics, Lund Observatory, Lund University, Box 43, SE-221 00 Lund, Sweden
[2]Department of Physics, Lund Institute of Technology, Box 118, SE-221 00 Lund, Sweden
[3]Department of Physics, Stockholm University, AlbaNova University Centre, SE-106 91 Stockholm, Sweden

Abstract

In dilute astrophysical plasmas, such as planetary nebulae and H II regions, strong lines appear that only have weak, if any, correspondence to the spectrum of laboratory light sources. Some of these are parity forbidden lines, i.e. emission from long-lived metastable states that cannot decay via normal electric dipole (E1) routes but only via the slower M1 and E2 transitions. The long lifetime of the upper levels and their sensitivity to collisions make the lines good diagnostics of the emitting plasma, but then the transition probability, or *A*-value, of these lines must be known.

We report on a technique to experimentally determine *A*-values for forbidden lines using the method of combining the lifetime of the upper level with the branching fractions for the different decay channels. The lifetime is measured using the laser probing technique (LPT) on a stored ion beam. Since these lines are rarely produced in laboratory plasmas, we use astrophysical spectra to determine the branching fractions (*BF*). The lifetime and the *BF* then give the *A*-value, which is one quantity needed for modeling the spectrum of the plasma emitting the forbidden lines.

The present measurements are performed within the FERRUM project, an international collaboration producing and evaluating transition probabilities for iron group element lines of astrophysical importance [Johansson, P. I. S. *et al.*, Physica Scripta **T100**, 71 (2002).]

1. Introduction

In the early days of spectroscopy, the spectrum of an astronomical object was compared with the spectrum of laboratory discharges of known elements and the coincidences in wavelength served as an identification tool. This technique, which basically still is used today in more refined ways, was successful in identifying most lines. However, some nebular lines remained unidentified until 1928 when Bowen [2] explained these lines as transitions between states of the same parity in doubly-ionized oxygen, [O III]. Following this discovery, Merrill identified [Fe II] lines in the spectrum of Eta Carinae and stated that

'*Astronomical observations may thus supplement those of laboratory by supplying data on line emission under very low densities*',

which is true for the present work, and also that

'*forbidden lines may thus perhaps yield information concerning conditions in the stars*' [3].

The work described in the present paper uses an astrophysical source, Eta Carinae, to determine atomic parameters, transition probabilities of forbidden lines, which cannot easily be measured in a laboratory.

The parity forbidden lines are M1 or E2 transitions between states of the same parity. The transition rates for these lines, about $1\,\mathrm{s}^{-1}$, are much lower than for ordinary E1 transitions, which have
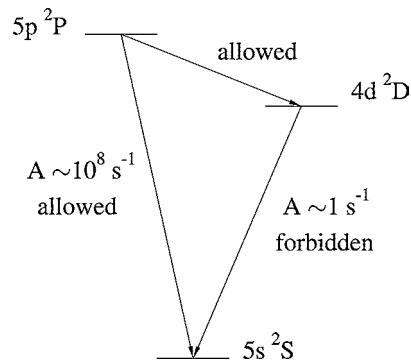
*Henrik.Hartman@astro.lu.se

Fig. 1. The lowest levels in Sr II. The transition rates from 5p and 4d, respectively, to 4s are indicated in the figure. The 5s-5p is an E1 transition whereas the 5s-4d is parity forbidden.

rates of $10^8\,\mathrm{s}^{-1}$. The forbidden transitions are thus most often negligible for most levels. For some levels there is no possible E1 decay, and for these levels the "forbidden" lines are the dominating radiative decay. This is the case for the lowest levels in many atoms and ions, where all have the same parity (see Figure 1). Many complex spectra have multiple metastable levels, e.g. Fe II has 62 metastable states. Since the decay is slow, the lifetime of these levels is long, of the order of seconds, compared to nanoseconds for most levels that decay via E1 transitions.

The collisional decay rate in most laboratory light sources is much larger than the radiative decay rate for metastable levels, which makes the forbidden lines too faint to be detected. But in dilute astrophysical plasmas, such as H II regions and planetary nebulae, the number density and the collision rate are low and the states can decay radiatively before being quenched (Figure 2 shows forbidden lines in Eta Carinae, observed by STIS onboard the *Hubble Space Telescope*). These objects have a low particle density with few collisions and are also large enough to produce visible forbidden lines.

The sensitivity to collisions for the metastable levels make the forbidden lines from the same ion but different levels useful for plasma diagnostic purposes. Line pairs in light elements are frequently used for determination of temperature and electron density. The density is determined using lines whose upper levels have about the same excitation energy, but different lifetimes. For temperature determination, lines from different excitation energies are used [4].

In the following section experimental transition probabilities for forbidden lines are discussed. The measurements of the lifetimes for complex ions used in the determination is described in section 3 and derivation of branching fractions in section 4.
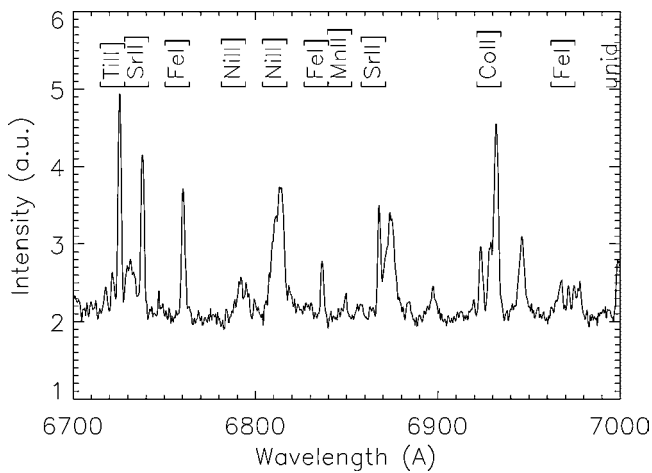
Fig. 2. HST/STIS spectrum of an ejecta close to Eta Carinae, called the Strontium Filament, showing forbidden lines from iron-group elements and Sr II [9].

In section 5 the resulting transition probabilities, *A*-values, and the uncertainty of these are discussed.

2. Transition probabilities

For the temperature and density determination using specific line pairs, and also for modeling of more complex spectra, one of the relevant atomic parameters entering the expressions is the transition probability of the lines. The vast majority of the *A*-values are produced by calculations. The amount of experimental data for forbidden lines is very limited, and concentrated to simple spectra. These are more easily measured due to the limited number of metastable levels and also few decay channels.

One way to determine experimental *A*-values is to combine the radiative lifetime of an upper level, τ_u, with the relative intensities, I_{ul}, for the decay from this level:

$$\tau_u = \frac{1}{\sum_l A_{ul}},$$

$$BF_{ul} = \frac{A_{ul}}{\sum_l A_{ul}} = \frac{I_{ul}}{\sum_l I_{ul}},$$

$$A_{ul} = \frac{BF_{ul}}{\tau_u}.$$

This approach is frequently used for E1 transitions, where the nanosecond-lifetime can be determined through e.g. laser induced fluorescence (LIF) and the branching fractions measured in the spectrum of a discharge lamp [1]. Lifetimes of metastable levels are in a totally different time domain and these are commonly measured using ion traps or storage rings, where the radiation is detected as the metastable levels decay.

Lifetime measurements of complex spectra, with large numbers of metastable levels, require an environment having few collisions and also need to be selective enough to measure only one level at a time.

We have used the advantages of the controlled low-density environment in an ion storage ring, in combination with the selectivity of the laser, to measure long metastable lifetimes for complex ions. A laser probing technique (LPT) developed at the CRYRING facility [5] by Mannervik and his group [6], first tried on simple spectra, has proven successful also in measuring lifetimes in complex spectra.

The relative intensity of the forbidden lines is derived from the spectrum of dilute plasmas of the object Eta Carinae. This object hosts good locations for studies of forbidden lines: spatially well-defined gas clouds that show rich emission line spectra with both allowed and forbidden lines. Lines from these regions are used to get the *BF*, and the measured lifetimes put the relative values on an absolute scale.

3. Lifetime measurements

The use of laser probing of a stored ion beam for lifetime measurements has been discussed and reviewed in a number of publications during the last years [6, 7, 8, 10, 11], and here will just be given an overview of the technique.

Storage rings can be used in passive measurements of metastable lifetimes. The ions are accelerated into the ring, most of them being in the ground state but some in excited, metastable states. When the excited ions decay the spontaneous emission is observed. As time passes the number of ions in the metastable state is reduced, and this is noticed as a decrease in the observed emission. The emitted light is observed in strong decay channels, and the lifetime is measured in real-time, see e.g. [12]. To gain statistics the procedure is repeated and the different curves are co-added.

This passive ion storage technique is only suitable for shorter lifetimes where the decay rate is higher, and cannot easily be used to measure longer lifetimes in ions having numerous metastable states. To measure lifetimes of metastable states in complex ions a selective technique is required, where the influence from the other levels can be minimized. The population is distributed among many levels, and the population in each level is small compared to ions with few metastable levels. The detection efficiency must therefore be increased. At the storage ring CRYRING (MSL, Stockholm), a laser probing technique (LPT) applied to a stored ion beam has been successfully developed for simpler spectra, such as Ca II and Sr II [13], which have only two metastable states. This method has proven to be suitable also for complex ions, such as the iron-group elements and the rare-earth elements, with many metastable levels. The LPT meets the requirements of selectivity and high efficiency: a single level can be measured using a tunable laser, and high detection efficiency is obtained by forcing the decay to appear in front of the photo-multiplier.

Instead of studying the spontaneous decay from the metastable state, and to passively monitor the lifetime, a laser pulse is used to deplete the state by photoexcitation to a higher level (Figure 3).
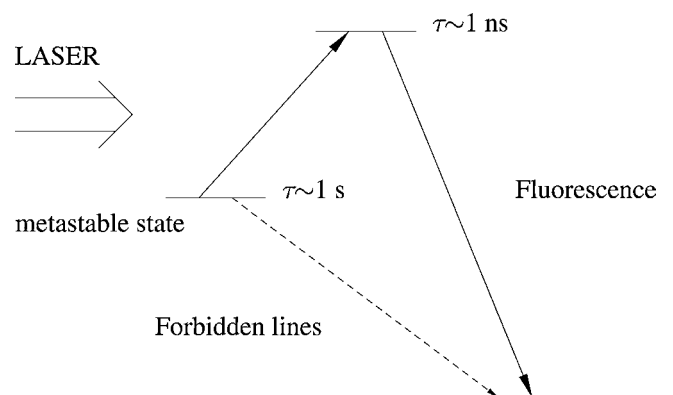

Fig. 3. Principle of the LPT. The metastable state is selectively pumped by a laser to an upper state, which decays promptly in the fluorescence channel. The fluorescence signal, observed in one or more lines, is proportional to the population in the metastable level. The spontaneous radiative decay from the metastable level is the forbidden lines observed in the spectrum of Eta Carinae.
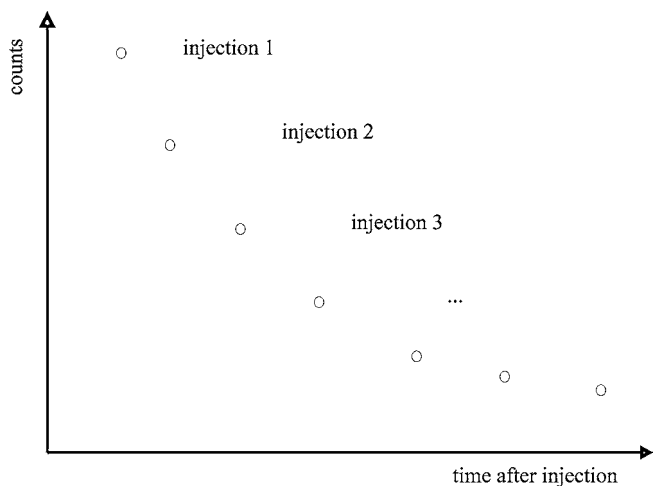
Fig. 4. Each ion injection gives a point on the lifetime curve. By varying the time delay for the laser pulse the decay curve is built up.

The applied laser wavelength is tuned to match a strong transition to the higher state. In this way most of the ions, being in the specific metastable state, are left in a higher excited state by absorbing the laser light. The higher state chosen should have a short lifetime and thus decay promptly in another channel. The intensity in this fluorescence signal is then a measure of the population in the metastable state. The method is destructive in the sense that all ions in the state under investigation are depleted and cannot be used for further measurements. A new bunch of ions has to be injected and stored in the ring.

By applying the laser pulse at different time delays after ion injection into the ring, the lifetime curve is built up (Figure 4). Each injection then gives one point on the lifetime curve. Since this technique is destructive the experiment requires stable beam conditions. All injections must be equal in terms of number of ions, and the fraction of metastable states may not vary too much. These properties of the ion beam are monitored, and if the conditions are not the same, then the various recordings are normalized.

Although the storage ring is evacuated to an extremely low pressure, below 10^{-11} mbar, the collisions with the rest gas affect the stored ions considerably. This is especially true for the longer lifetimes. Important processes are shown in Figure 5. The observed decay curve has to be corrected for collisional excitation and deexcitation. The former is measured separately by first emptying the state and monitoring the re-excitation. The deexcitation is measured by changing the pressure in the ring and deriving a collisional decay rate that is subtracted from the observed decay. The details of these processes and how they are corrected are given in earlier publications [6, 7, 8, 10, 11] .
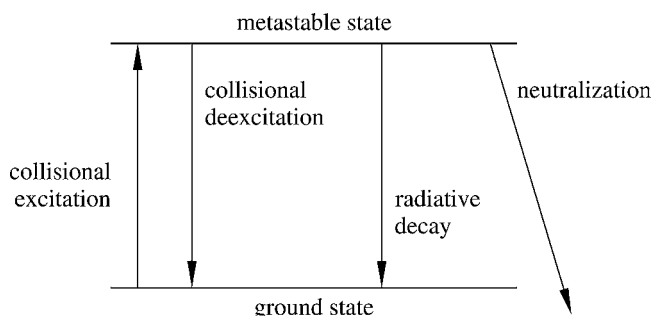

Fig. 5. Many processes affect the population in the excited state. The relevant property is the radiative decay while the others are minimized and corrected for.

4. Astrophysical branching fractions

The branching fractions for forbidden lines cannot easily be measured from ordinary laboratory sources simply because strong forbidden lines are not produced in them. The metastable levels are collisionally deexcited on a shorter timescale than the radiative decay. If the forbidden lines are to be observed the density must be very low. Under these circumstances the number of atoms in any state is low and the radiation will be very weak. To get a strong emission the number of ions in the specific state must be large, and together with a low density, a large volume is needed. This can be achieved in thin astrophysical plasmas like planetary nebulae and H II regions, which show strong forbidden lines. Low density plasmas around stars may also show emission lines, also from heavier elements which normally are not observed in emission from nebulae. A spectrum of an ejecta from the massive star Eta Carinae is shown in Figure 2. Different parts of the Eta Carinae nebula show different line spectra but have in common strong emission lines, both forbidden and allowed, which are spatially well-defined.

The use of astrophysical lines for measurement of relative intensities have some additional problems compared to laboratory measurements. The spectral resolution is often lower and several regions along the line of sight are observed, the problems with line blending and broadening is thus more problematic. Another disadvantage is that the physical conditions and relative abundances are fixed and cannot be optimized as in a laboratory.

On the other hand, forbidden lines are rarely produced in laboratory sources. The spectra for the emission line regions we have used to derive the branching fractions (i.e. the Weigelt blobs and the Sr-Filament of Eta Carinae) are previously analyzed in detail and therefore well known [9, 14]. The careful analysis of the whole spectrum gives confident line identifications and lines with large blends can be corrected for or avoided.

The property needed for the branching fractions is the intrinsic line ratio, i.e. the ratio between the lines at the point of emission. This is not the same as the line ratio we measure, since the light is scattered on its way from the emission gas cloud to the telescope and the scattering is wavelength dependent. In the interstellar medium, blue light is more scattered out of line of sight than red light and this effect is therefore often referred to as reddening. The observed line ratios must be corrected for reddening to get the true intrinsic line ratio, the branching ratio. The shape of the scattering as a function of wavelength, $f(\lambda)$, is observed to have the same shape in the direction of most stars according to

$$\frac{I_{\lambda_1}}{I_{\lambda_2}} = \frac{I_{\lambda_1,0}}{I_{\lambda_2,0}} \cdot e^{-C[f(\lambda_1)-f(\lambda_2)]}$$

where C is a constant related to how much material lies between the star and the observer [4]. The amount of scattering, C, is dependent on the amount of material along the line of sight and varies for different directions and has to be determined for each object. Thus, by assuming the standard function of the reddening for $f(\lambda)$, and if the amount of reddening C is known, the ratio of the lines investigated can be 'de-reddened'. C for emission line objects is best determined from lines with known intrinsic intensity ratios. Lines from the same upper level and with known A-values are especially well suited for this, since no assumption about the relative level population is needed.

A problem involved in branching fraction measurements of parity allowed lines (E1) is self-absorption, i.e. the emission line is absorbed by the same transition during transfer in the plasma.

Since the transition probability for the forbidden lines is very low, this effect is negligible.

All lines from an upper level can usually not be measured. Lines can be outside the observed wavelength region or too faint to be measured. Since $BF_{ul} = I_{ul}/\sum_l I_{ul}$, it requires that the intensities of all transitions from the upper level have to be estimated. The residual, defined as the line intensity that cannot be measured, can be derived from calculations. If the missing lines are too weak or blended, an upper estimate can be given and checked against the calculation. But, due to the uncertainty of the calculations, if a large amount of the intensity falls outside the observed region, no reliable BF can be derived from that level.

5. Uncertainties and resulting *A*-values

The sources of uncertainty for the astrophysical BF are calibration of the instrument, intensity measurements, residual and reddening determination. The uncertainty for the latter depends on the wavelength span of the emission lines. For levels which have decays in different wavelength regions, the uncertainty in the reddening correction is the major source, whereas for lines within a limited range, and assuming a standard reddening curve, the difference in reddening is small.

The uncertainty in the lifetime measurements comes from the fit of the lifetime curve and, more important, the corrections for collisional excitation and deexcitation. The total uncertainty for the *A*-values is in the range 10–40%, where the smaller uncertainty applies to strong lines that fall in the same wavelength region, and the larger for weaker lines with a large spread in wavelength for the different branches and therefore a larger correction for reddening. The contribution to the total uncertainty from the branching fractions is larger compared to the contribution from the lifetime measurements.

Due to the time consuming technique for the lifetime measurements, and the limited number of forbidden lines showing up in spectra, the majority of the *A*-values must be supplied by calculations and not by experiment. The experimental values can, on the other hand, be derived with uncertainties and then compared to theory. In Figures 6 and 7 the results of lifetime measurements and derived *A*-values, respectively, for Fe II [10, 16] are compared to the calculation by Quinet [17], which is the calculation that show best agreement with our experimental values. See also Tables I and II. The $b^2H_{11/2}$ level is mixed with $a^4G_{11/2}$ which has similar energy. This might be the reason for the difference in the values for this level since the lifetime is very sensitive to the mixing.
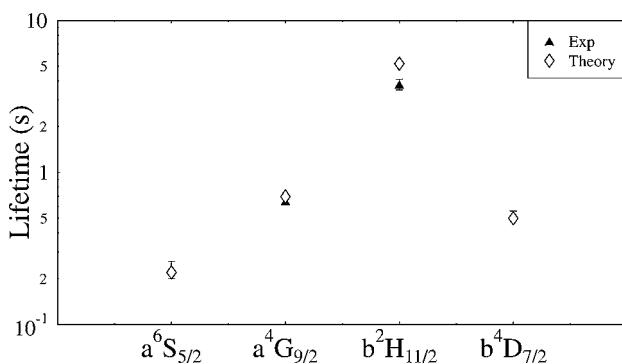

Fig. 6. Experimental lifetimes with error bars for Fe II levels [16, 10]. The theoretical values are from Quinet *et al.* [17], which are the calculations that show the best agreement with experiment.
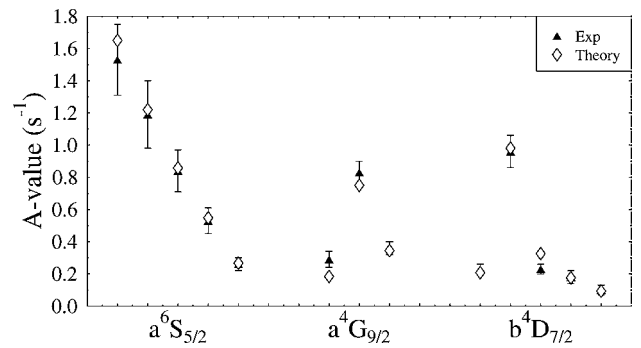
Fig. 7. Experimental *A*-values with error bars for forbidden [Fe II] lines [10]. They are compared to theoretical values from Quinet *et al.* [17].

Table I. *Experimental lifetimes for metastable levels in Fe II and Ti II.*

	level	lifetime (s)	ref.
Fe II	$a^6S_{5/2}$	0.23 (3)	[16]
	$a^4G_{9/2}$	0.65 (2)	[10]
	$b^2H_{11/2}$	3.8 (3)	[10]
	$b^4D_{7/2}$	0.53 (3)	[16]
Ti II	$b^4P_{5/2}$	28 (10)	[11]

Table II. *Experimental A-values for forbidden [Fe II] lines (from [10]).*

Upper level	Lower level	λ_{vac} (Å)	A (s^{-1})
$a^6S_{5/2}$	$a^6D_{9/2}$	4288.60	1.53 (0.22)
	$a^6D_{7/2}$	4360.56	1.19 (0.21)
	$a^6D_{5/2}$	4415.02	0.84 (0.13)
	$a^6D_{3/2}$	4453.35	0.53 (0.08)
	$a^6D_{1/2}$	4476.16	0.26 (0.04)
$a^4G_{9/2}$	$a^4F_{9/2}$	4178.37	0.29 (0.05)
	$a^4F_{7/2}$	4278.03	0.83 (0.07)
	$a^4F_{5/2}$	4354.00	0.36 (0.04)
$b^4D_{7/2}$	$a^6D_{9/2}$	3176.30	0.23 (0.03)
	$a^4F_{9/2}$	3377.17	0.96 (0.10)
	$a^4F_{7/2}$	3441.98	0.23 (0.03)
	$a^4P_{5/2}$	5552.85	0.18 (0.04)
	$a^4P_{3/2}$	5614.83	0.10 (0.03)

6. Conclusion

Since parity forbidden lines almost exclusively are observed in astrophysical spectra, there is no straightforward way to measure the *A*-values for these lines using a laboratory source. Still, the transition probabilities are needed for diagnostics and modeling of these lines in low density plasmas. To derive experimental transition probabilities for forbidden lines we combine the lifetime of the upper level with the branching fractions of the decays from this level.

The lifetime is measured using a laser probing technique on a stored ion beam. The low pressure minimizes the collisional destruction from other ions and allow to measure long metastable lifetimes. The laser probing provides the selectivity needed and increases the detection signal with several orders of magnitude.

The branching fractions are derived from emission line *HST*/STIS-spectra of ejecta close to the massive star Eta Carinae. These regions host the conditions to produce strong forbidden lines from the interesting levels. We have measured lifetimes from metastable levels in Fe II and Ti II and derived transition probabilities for [Fe II] and [Ti II] lines.

Acknowledgement

References

1. Johansson, S. *et al.*, 2002, Physica Scripta **T100**, 71 (2002).
2. Bowen, I. S., Astrophys. J. **67**, 1 (1928).
3. Merrill, P. W., Astrophys. J. **67**, 391 (1928).
4. Osterbrock, D., "Astrophysics of Gaseous Nebulae and Active Galactic Nuclei" (University Science Books, California 1989).
5. Abrahamsson, K. *et al.*, Nucl. Instr. Meth. Phys. Res. B **79**, 269 (1993).
6. Mannervik, S., Physica Scripta **T100**, 81 (2002).
7. Ellmann, A., Ph.D thesis, Stockholm University (2003).
8. Hartman, H., Ph.D thesis, Lund University (2003).
9. Hartman, H., Gull, T., Johansson, S., Smith, N. and HST Eta Carinae Treasury Project Team. Astron. Astrophys. **419**, 215 (2004).
10. Hartman, H. *et al.*, Astron. Astrophys. **397**, 1143 (2003).
11. Hartman, H. *et al.*, J. Phys. B: At. Mol. Opt. Phys. **36**, L197 (2003).
12. Träbert, E. *et al.*, J. Phys. B: At. Mol. Opt. Phys. **36**, 1129 (2003).
13. Lidberg, J. *et al.*, Nucl. Instr. Meth. Phys. Res. B **152**, 157 (1999).
14. Zethson, T., Ph.D thesis, Lund University (2001).
15. Smith, N. *et al.*, Astrophys. J. **605**, 405 (2004).
16. Rostohar, D. *et al.*, Phys. Rev. Lett. **86**, 1466 (2001).
17. Quinet, P., Le Dourneuf, M. and Zeippen, C. J., Astron. Astrophys. suppl. **120**, 361 (1996).